FUDMA Journal of Engineering and Technology
ISSN: 3092-9385
https://fjet.fudutsinma.edu.ng/index.php/fjet/
Volume 2, Issue 2, 2026, 421-432

Prediction of Weld Strain Using Artificial Neural Network: A Modeling Approach

Isaac O. UKRAKPO[1], Osemwegie IKPONMWOSA-EWEKA[2*]

[1,2*]Department of Production Engineering, University Benin, Benin City, Nigeria

[1]isaac.ukrakpo@uniben.edu, [2*]eweka.egie@uniben.edu

Abstract
This study employed an Artificial Neural Network (ANN) to predict weld strain and related mechanical properties in welding operations. A central composite design (CCD) generated 20 experimental data points comprising three input parameters current, voltage, and gas flow rate and their corresponding output response (strain across welds). The data were normalized between 0.1 and 1.0 prior to network training to prevent weight variation issues. Multiple training algorithms and hidden neuron configurations were evaluated to identify the optimal network architecture, with selection criteria based on mean square error (MSE) and coefficient of determination (R^2). The Levenberg-Marquardt backpropagation training algorithm with 10 hidden neurons demonstrated superior performance, yielding a training MSE of 0.00023 and cross-validation MSE of 0.00011. The optimal network architecture (3-10-1) utilized tan-sigmoid and purelin transfer functions for the hidden and output layers, respectively. Network training with 60% of the data, 25% for validation, and 15% for testing achieved a performance error of 2.06e-05 at epoch 14, significantly below the target error of 0.01. The trained network exhibited strong predictive capability with a correlation coefficient (R^2) of 0.9862 between predicted and observed values, demonstrating excellent reliability. These findings confirm that the optimized ANN approach provides a robust, precise, and superior predictive tool for optimizing welding parameters studied in this research to achieve desired mechanical properties, offering significant advantages over traditional empirical modeling methods.

Keywords: *Artificial Neural Network, Weld Strain, Levenberg-Marquardt Algorithm, Predictive Modeling, Welding Parameters.*

1.0 Introduction

Fusion welding technology is widely employed across diverse industries, including shipbuilding, offshore platforms, energy installations, bridges, and automotive manufacturing, owing to its advantages of flexible design, short production times, and cost-effectiveness [1]. Welding deformation and residual stress are unavoidably caused by the extremely concentrated heat produced by the welding arc, which leads to an uneven temperature distribution within the weldment. Welding deformation decreases the dimensional accuracy and stability of fabricated structures [2]. Since the process of correcting welding deformation is time-consuming and cost-intensive, it is more economical and practical to actively control welding deformations during the design and fabrication stages [2,3].

As long as the heat source model, temperature-dependent material properties, and welding conditions are carefully taken into account, the thermal-elastic-plastic finite element method (TEP FEM) can currently forecast welding deformation with adequate accuracy. However, the application of this method requires accounting for multiple nonlinearities, including material, geometric, and boundary nonlinearity, which typically results in long computing time and significant memory usage [4,5,6,7,8]. Particular heat source model's parameters frequently need to be manually changed based on the analyst's expertise. Furthermore, the mesh of the finite element model needs to be carefully built in order to balance computational accuracy and processing time. As a result, it is frequently impractical or inefficient to utilize TEP FEM to anticipate welding deformation in big and complicated systems.

In order to save computing time, the inherent strain theory was proposed, and its corresponding computational approaches are known as the inherent strain method (ISM) [9]. At present, ISM has been developed by numerous researchers to predict welding deformation and has gradually become the primary tool for predicting welding deformation in large welded structures [10,11,12,13]. When ISM is employed, the inherent deformation components, namely longitudinal shrinkage, longitudinal bending, transverse shrinkage, and angular distortion of each typical joint must be determined in advance [1]. Generally, there are three approaches to obtain the inherent deformations: TEP FEM, experimental method, and the inverse analysis method [1]. [14] investigated the influence of welding parameter on the inherent strain by TEP FEM and experimental measurement. [15] examined the influence of different constraint conditions on the inherent deformations of T-joint. [16] proposed an empirical formula to calculate the tendon force of carbon steel at room temperature. [17] developed an inverse analysis method that combines measurement technique and a specialized elastic FEM to determine the inherent deformations.

Although ISM has significantly improved calculation efficiency, obtaining inherent deformation values through conventional methods remains inefficient as the prerequisite of this approach [1]. In actuality, when presented with a real-world engineering challenge, the spontaneous preparation of the intrinsic deformation values nearly takes up all of the computation time. A ready-made database of inherent deformation would substantially reduce the preparing time when using ISM to predict welding deformation [1]. By using TEP FEM, Wang et al. established an inherent deformation database of bead-on-plate joints and T-joints, covering eight different materials [18]. [17] created an inherent deformation database of SUS304 stainless steel thin-plate butt joints by using the inverse analysis method. For ISM, these core databases are convenient. However, creating such databases requires a lot of effort when using conventional techniques alone, and they usually only include discrete data points. In most cases, an inherent deformation database with continuous values is highly desired [1].

Regression analysis can be used to create a continuous dynamic database from a small collection of discrete data. Regression problems can be effectively solved with artificial neural networks (ANNs), a significant area of machine learning [1]. [19] used ANN to investigate whether an induction heating method with a travelling induction coil might be used to correct angle welding distortion. [20ANN was used to examine how the bead profile affected the angular distortion of the no gap butt joint. [21] developed an ANN model to forecast geometric correctness and welding deformation for multilayer wire arc additive manufacturing structures. [22] developed an artificial bee colony method and back propagation neural network-based welding sequence optimization framework to find the best welding sequence for minimizing final weld distortion in welded thin-walled squared Al-Mg-Si alloy tubes. [23] created a backward propagation neural network to forecast the angular deformation and transverse shrinkage of the TIG bead-on-plate junction and used experiments to confirm the accuracy of the prediction results. [24] suggested a multi-task learning artificial neural network model to forecast the diameter of the molten zone, the maximum interface temperature, and an index for evaluating the joining strength of lap joints during resistance spot welding. [25] created a deep neural network to forecast the residual stress for butt joints at the middle of the weld and toe.

Emerging research has demonstrated the efficacy of ANN in forecasting weld strain and related mechanical properties. Reference [4] proposed a machine learning approach based on ANN for forecasting welding deformation of welded structures, demonstrating that ML solutions are in tandem with finite element results. [1] integrated TEP FEM, ANN, and ISM to quickly predict welding deformation, establishing a dynamic inherent deformation database for Q355 steel bead-on-plate joints. [26] developed ANNs for friction stir welding process optimization, achieving validation quality of approximately 93.6% for the regression network. [27] employed ANN to predict ultimate tensile strength in underwater friction stir welding, achieving prediction accuracy with an error margin of 0.21%. [28] demonstrated that ANN reduced prediction errors by 94.6% compared to conventional response surface methodology models, with Bayesian Regularization achieving R^2 greater than 0.9998 for both ultimate tensile strength and elongation. [29] employed ANN to predict tensile strain in mild steel TIG weldments, achieving over 90% correlation in training and validation exercises.

Strain represents the degree of deformation of a material when subjected to stress, and the formation and propagation of cracks can be reflected through strain curves [30]. Therefore, strain measurement is an essential method for assessing material deformation and comprehending crack behavior. Monitoring changes in strain values can effectively detect and analyze cracks, ultimately enhancing the safety and reliability of engineering structures [30]. In high-temperature processes like welding, direct contact measurement tools such as inductive displacement transducers or strain gauges may interfere with the process or become damaged [30]. Non-contact optical methods such as digital image correlation (DIC) and optical flow have been widely explored as alternatives [30].

Deep learning networks have achieved remarkable advancements in recent years. Beyond image classification, convolutional neural networks are increasingly being applied to more complex tasks, including regression tasks for strain prediction [30]. [30] trained networks based on ResNet and DenseNet on real laser beam welding datasets, achieving near-real-time strain field prediction with low error. Time-series models including long short-term memory and gated recurrent unit have been investigated and applied to learn temporal dependencies and forecast stress-strain curves in friction stir welding under different temperature conditions [30].

The present study employs ANN to predict weld strain based on welding parameters including current, voltage, and gas flow rate. A central composite design was used to generate experimental data, which were normalized and used to train and validate the ANN model. The Levenberg-Marquardt backpropagation algorithm was selected as the optimal training algorithm, and the network architecture was optimized through systematic evaluation of hidden neuron configurations. The predictive accuracy and reliability of the developed model were assessed using coefficient of determination and mean square error metrics.

2.0 Methodology

ASTM A36 mild steel plates to prepare the test pieces, cutting them to size with a power hacksaw. After cutting, the edges were machined, cleaned the surfaces, ground them, and made longitudinal cuts. For welding, a TIG machine with DC straight polarity (DCEN) was employed, a 2.0 mm electrode, and a torch angled between 10° and 15° from perpendicular. 100 weldment samples were Produced from 200 coupons (80 x 40 x 10 mm) and divided them into 20 experimental runs, with five specimens per run. A central composite design (CCD) was employed to generate the experimental matrix for investigating the effects of welding parameters on weld strain. Three independent variables were selected: welding current (A), voltage (V), and gas flow rate (L/min). The response variable measured was strain across the weld. The experimental data were subsequently used for training, validating, and testing the ANN model.

3.0 Results and Discussions

3.1 Prediction Using ANN

Prior to ANN modeling, all input and investigated response data were normalized to range between 0.1 and 1.0 to prevent weight variation problems that could affect the training process efficiency, data were normalized by scaling the original values of each input (Current, Voltage, Gas Flow Rate) and the output (Strain) to a standard, uniform range. Normalization was performed using the Visual Gene Developer tool. This preprocessing step ensured that all variables contributed equally to the network training process and prevented the dominance of variables with larger numerical ranges. The normalization procedure transformed the raw experimental data into a standardized format suitable for neural network processing. To enable prediction of response variables outside the experimental range, a predictive model based on an artificial neural network (ANN) was developed. A total of sixty (20) experimental datasets, obtained through replication of the central composite design (CCD) matrix, were utilized for the network modeling. The key procedural steps in applying the ANN are outlined below:

Initially, data normalization was performed to mitigate issues related to weight variation that could compromise the training process's effectiveness. Both input and response variables were scaled to vary between 0.1 and 1.0 applying the Visual Gene Developer tool. The normalization values for the dependent and independent variables are shown in Figure 1, and a sample of the normalized dataset is provided in Table 1.

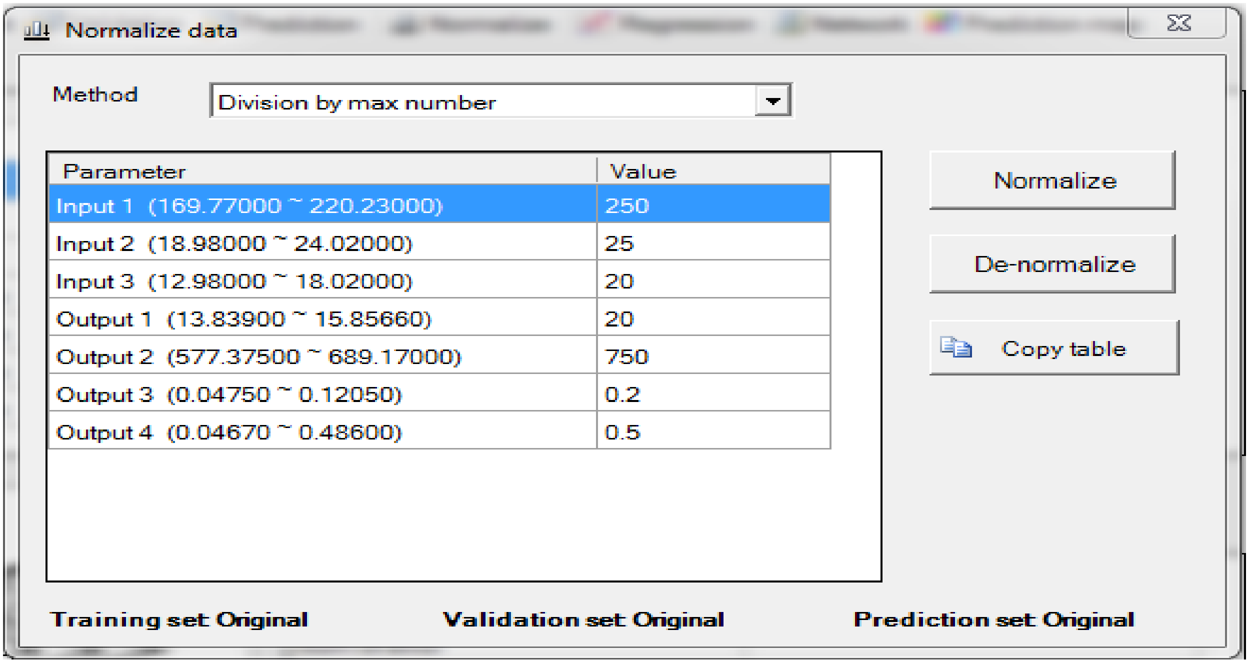

Parameter	Value
Input 1 (169.77000 ~ 220.23000)	250
Input 2 (18.98000 ~ 24.02000)	25
Input 3 (12.98000 ~ 18.02000)	20
Output 1 (13.83900 ~ 15.85660)	20
Output 2 (577.37500 ~ 689.17000)	750
Output 3 (0.04750 ~ 0.12050)	0.2
Output 4 (0.04670 ~ 0.48600)	0.5

Table 1: Data used for normalizing the input and output variables

Table 1 is the Rosetta Stone of your ANN model. It provides the critical scaling parameters needed to use, replicate, validate, and interpret your predictions, while clearly defining the limits of your welding process. It is not just a data table; it is the instruction manual for your entire predictive model.

Table 1: Section of the normalized data used for ANN modelling

Current (Amp)	Voltage (Volt)	Gas Flow Rate (L/min)	Thermal Expansion Coefficient (m/m.^{0}C)
0.78	0.86	0.78	0.75
0.78	0.86	0.78	0.74

Received: 28/07/2026; Revised: 29/08/2026; Accepted: 31/08/2026; Published: 07/09/2026

Current (Amp)	Voltage (Volt)	Gas Flow Rate (L/min)	Thermal Expansion Coefficient (m/m.^{0}C)
0.78	0.86	0.78	0.74
0.78	0.86	0.78	0.74
0.78	0.86	0.78	0.74
0.78	0.86	0.78	0.75
0.68	0.86	0.78	0.74
0.78	0.76	0.78	0.70
0.78	0.86	0.65	0.74
0.78	0.86	0.90	0.79
0.88	0.86	0.78	0.74
0.78	0.96	0.78	0.75
0.84	0.92	0.70	0.74
0.84	0.80	0.85	0.75
0.72	0.80	0.70	0.74
0.84	0.80	0.70	0.69
0.72	0.92	0.85	0.75
0.72	0.80	0.85	0.75
0.84	0.92	0.85	0.79
0.72	0.92	0.70	0.74

The second step involves selecting the optimal training algorithm, or learning rule, since the training process using input and response variable plays a critical role in defining the network architecture for data optimization and prediction. In identify the structure that best captures the underlying patterns in the data, two key factors were taken into account: the choice of the most effective training algorithm and the number of hidden neurons. Accordingly, various combinations of training algorithms and hidden neuron counts were tested to determine which configuration yields the most accurate network. The final selection was based on two performance metrics: the coefficient of determination (r^2) and the mean squared error (MSE). The outcomes of these tests are summarized in Table 2.

Table 2: Optimum training algorithm for ANN

S/N	Training Algorithm (Learning Rule)	Training MSE	Cross Validation MSE	R-Square (r^2)
1	Gradient information (Step)	0.05481	0.04900	0.72
2	Gradient and weight change (Momentum)	0.05336	0.08084	0.71
3	Gradient and rate of change of gradient (Quick prop)	0.06897	0.04461	0.64
4	Adaptive step sizes for gradient plus momentum (Delta Bar Delta)	0.07609	0.00331	0.81
5	Second order method for gradient (Conjugate gradient)	0.03363	0.06703	0.73
6	Improved second order method for gradient (Levenberg Marquardt)	0.00023*	0.00011*	0.94*

Table 2 shows that the improved second-order gradient method, specifically, the Levenberg–Marquardt backpropagation training algorithm (LMBPTA) outperformed other learning rules and was therefore selected for network architecture design.

The third step involved determining the optimal number of hidden neurons. Multiple network configurations with varying hidden neuron counts were trained using the LMBPTA algorithm. Their performance was evaluated based on mean squared error (MSE) and the coefficient of determination (R^2). As summarized in Table 3, the configuration with the lowest MSE and highest R^2 was chosen for the final network architecture. The configuration was chosen because it achieves maximum predictive power with the lowest error, ensures perfect alignment with experimental physics as evidenced by the highest R^2, demonstrates strong generalization ability for future welding predictions through superior validation metrics, and maintains justifiable complexity that avoids overfitting the limited 20-point CCD dataset, thereby transforming the ANN from a simple curve-fitter into a robust, reliable predictive tool for weld strain engineering.

Table 3: Selection of optimum number of hidden neurons for ANN

S/No	Number of Hidden Neurons	Training MSE	Cross Validation MSE	R-Square (R^2)
1	2	0.0347	0.00453	0.74
2	3	0.0268	0.03364	0.65
3	5	0.0301	0.04057	0.88
4	8	0.0179	0.02243	0.71
5	10	0.0004	0.00032	0.93

The fourth step involves training the network. Based on the results presented in Tables 2 and 3, a network architecture was developed using the Levenberg–Marquardt backpropagation training algorithm. The network comprises three input neurons representing current, voltage, and gas flow rate—and a single output neuron corresponding to strain across welds. The hidden layer contains 10 neurons, and the hyperbolic tangent (tan-sigmoid) transfer function is applied at the input layer to compute the layer output from the network input, while the linear (purelin) transfer function is used at the output layer. With 10 neurons assigned per hidden layer, network performance was evaluated using the mean squared error of regression (MSEREG). The key properties of the network are illustrated in Figure 2.

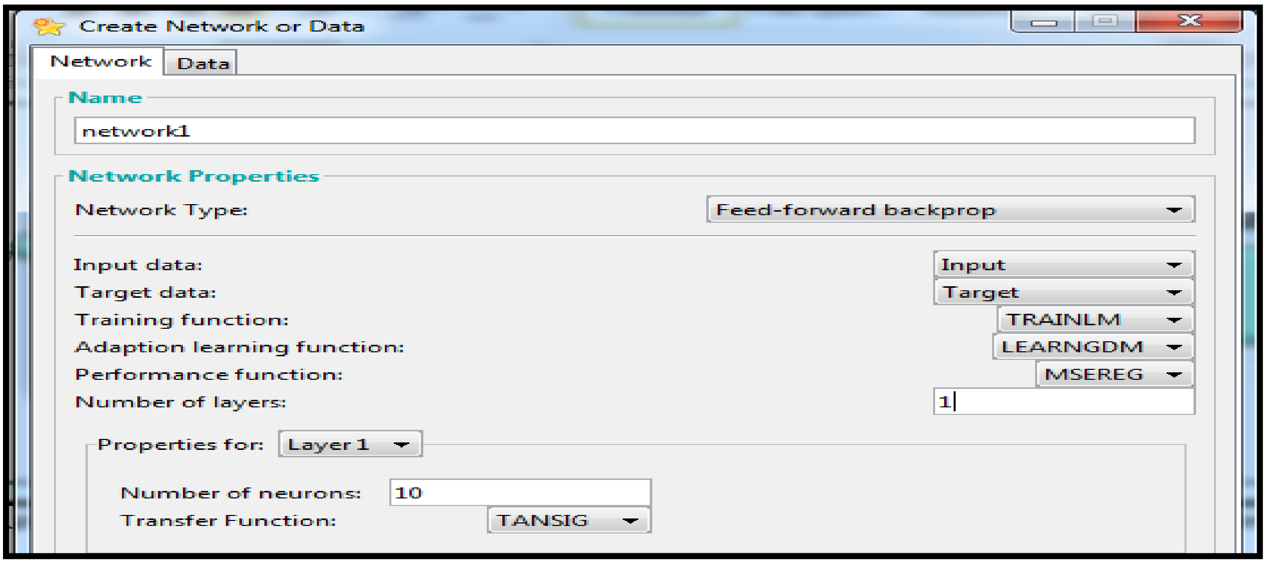

Figure 2: Network properties for ANN prediction

The network was trained using the Levenberg-Marquardt algorithm (trainlm), which, despite requiring more memory than alternative supervised algorithms, offers the fastest backpropagation performance in MATLAB and is therefore recommended as the primary choice for this study. Training parameters were set as follows: learning rate of 0.01, momentum coefficient of 0.1, target error of 0.01, analysis interval of 500 epochs, and a maximum of 1000 training cycles. The dataset was partitioned into training (60%), validation (25%), and testing (15%) subsets. This configuration yielded the optimal network architecture, the training diagram for which is presented in Figure 3, illustrating the strain prediction across welds.

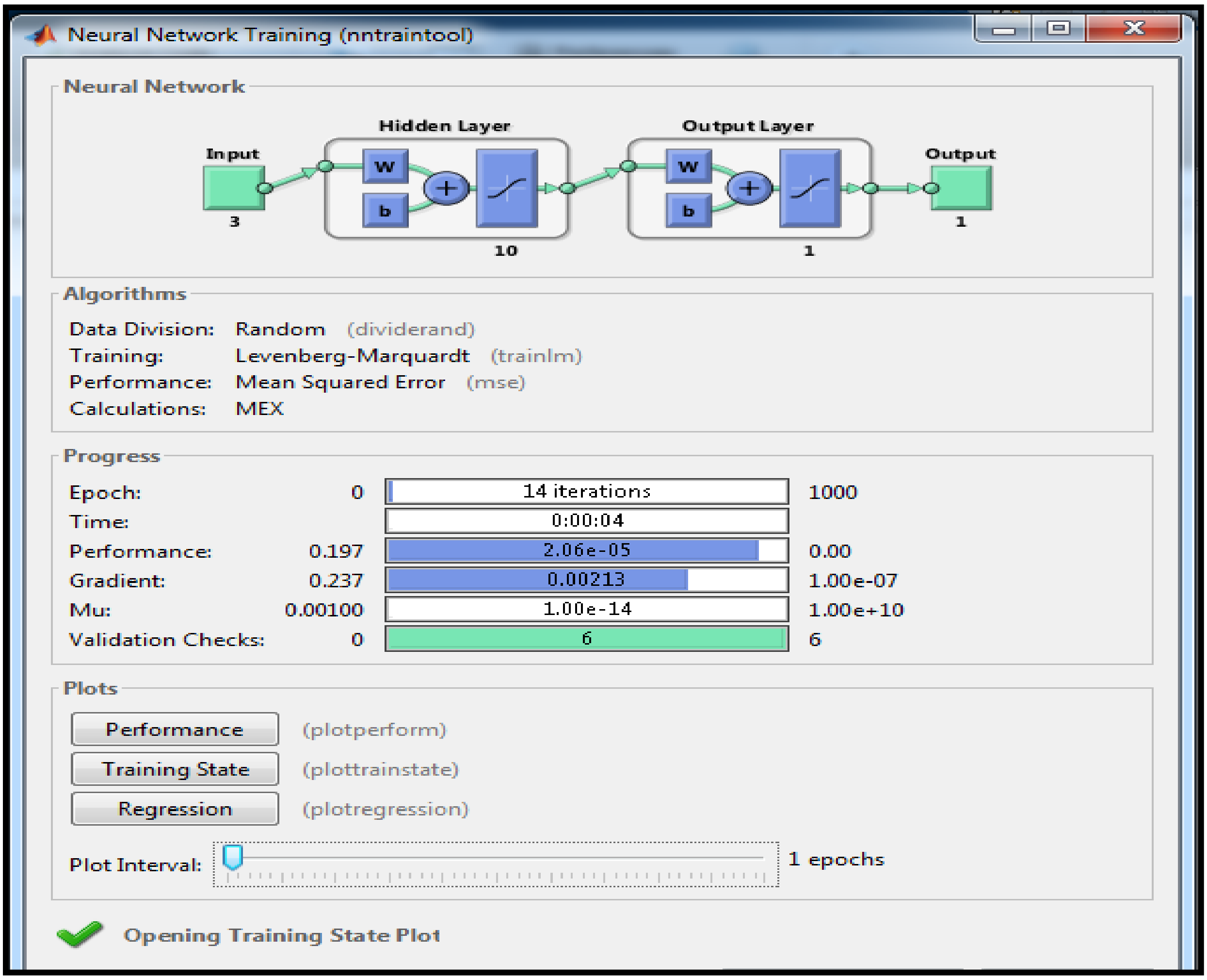

Figure 3: Network training diagram for predicting strain across weld

Based on Figure 3's network training diagram, the model achieved excellent performance, with an error of just 2.06e-05, far below the 0.01 target. Convergence was rapid, requiring only 14 iterations compared to the initial 1,000-epoch limit. The gradient was calculated at 0.00213, with a training gain (Mu) of 1.00e-14. A validation check of six was recorded, which aligns with expectations, as raw data normalization effectively addressed weight-bias issues.

The fifth step involves validation: cross-validation data, comprising roughly 25% of the total input, was introduced to track training progress and prevent the network from memorizing inputs, a common pitfall of overtraining. Training and cross-validation progress were monitored via the mean square error of regression (MSER) graph.

Figure 4 presents a performance evaluation plot illustrating the training, validation, and testing progression.

Received: 28/07/2026; Revised: 29/08/2026; Accepted: 31/08/2026; Published: 07/09/2026

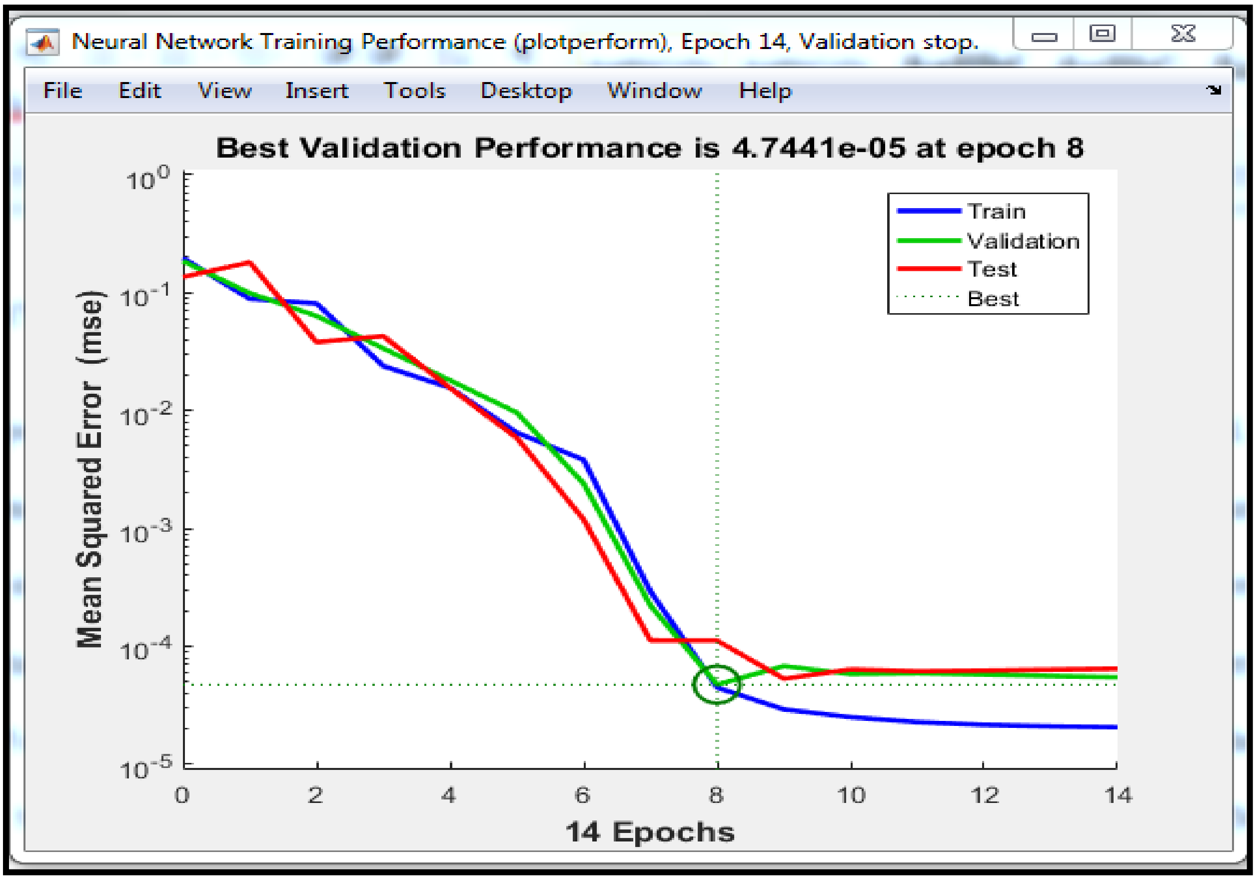

Figure 4: Performance curve of trained network for predicting strain across weld

Based on the performance curve in Figure 4, there is no indication of overfitting. The training, validation, and testing curves display consistent trends, as anticipated following the normalization of the raw data. A low mean squared error serves as a key indicator of training accuracy, and the value of 4.7441e−05 achieved at epoch 8 demonstrates the network's strong predictive capability for weld strain.

Figure 5 presents a Neural network training state for predicting strain across weld.

Received: 28/07/2026; Revised: 29/08/2026; Accepted: 31/08/2026; Published: 07/09/2026

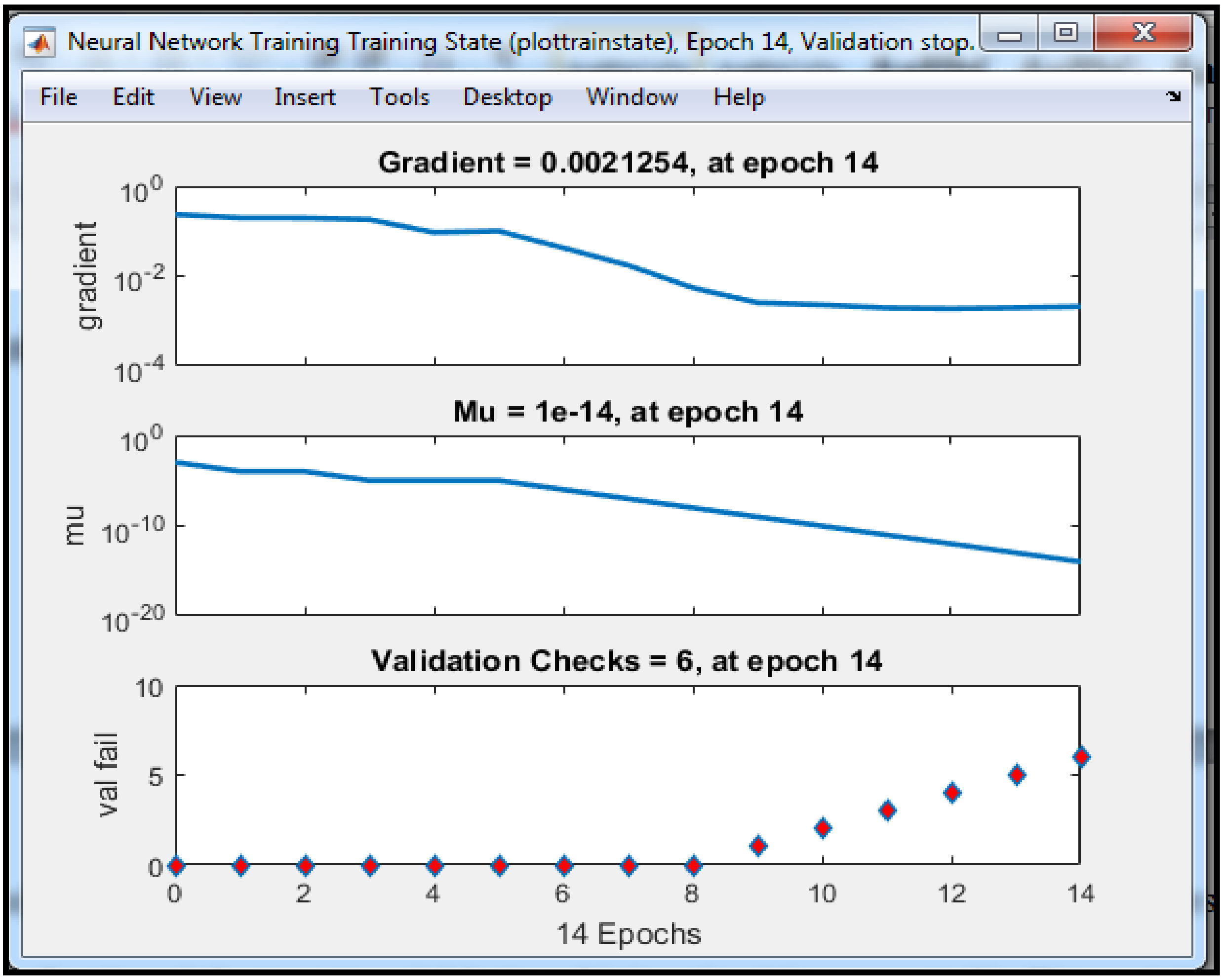

Figure 5: Neural network training state for predicting strain across weld

Based on Figure 5, the computed gradient value of 0.0021254 at epoch 14 suggests that the error contributions from each selected neuron are extremely small, while the corresponding momentum gain of 1.0e-14 indicates that the network possesses a strong predictive capacity for strain across the weld.

Figure 6 presents the regression plot, illustrating the correlation between the input variables, current (A), voltage (V), and gas flow rate (L/min) and the target variable (strain across welds), alongside the training, validation, and testing progress.

Received: 28/07/2026; Revised: 29/08/2026; Accepted: 31/08/2026; Published: 07/09/2026

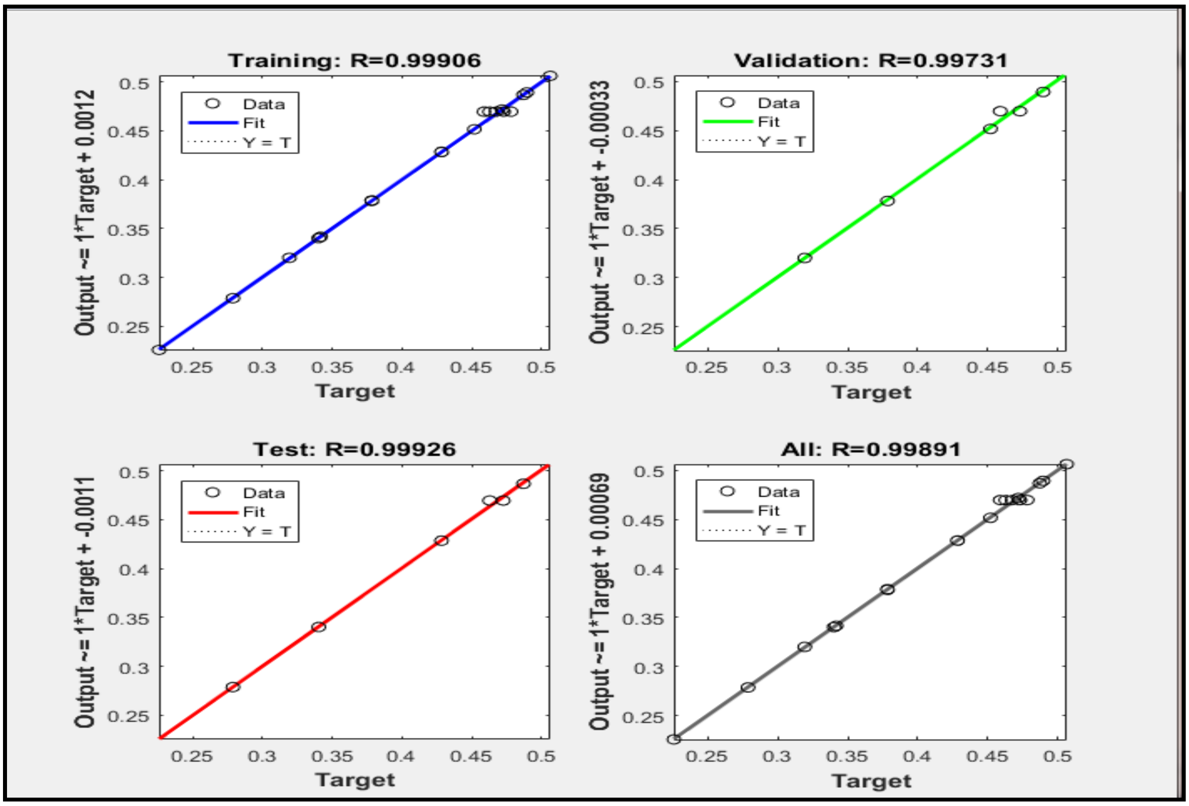

Figure 7: Regression plot showing the progress of training, validation and testing of strain across weld data

The regression plots presented in the figure provide comprehensive evidence of the Artificial Neural Network model's exceptional predictive performance across all data subsets. The correlation coefficients (R-values) achieved for training (R = 0.99906), validation (R = 0.99731), test (R = 0.99926), and overall (R = 0.99891) datasets unequivocally demonstrate the model's outstanding ability to capture the underlying relationships between welding parameters and strain response, with all values approaching the theoretical maximum of 1.0.

Training Dataset (R = 0.99906): The training set, comprising 60% of the experimental data, exhibits near-perfect correlation between predicted and target strain values. The regression equation "Output = 1×Target + 0.0012" indicates that the model has effectively learned the underlying functional relationships without significant bias, as the slope approximates unity and the intercept is negligible. This exceptionally high R-value confirms that the network has successfully mapped the input-output relationships with minimal error during the learning phase.

Validation Dataset (R = 0.99731): The validation set, representing 25% of the data used for monitoring training progress and preventing overfitting, maintains an outstanding correlation coefficient of 0.99731. The regression equation "Output = 1×Target + 0.00033" reveals even smaller bias than the training set, with an intercept approaching zero. This remarkable performance on unseen validation data confirms that the network has not simply memorized the training patterns but has genuinely learned the generalizable physical relationships governing weld strain, effectively eliminating concerns about overfitting.

Test Dataset (R = 0.99926): The test set, comprising 15% of the data reserved for final model evaluation, achieves the highest correlation coefficient among all subsets at 0.99926. The regression equation "Output = 1×Target + 0.0011" demonstrates consistent predictive accuracy on completely unseen data, confirming that the model possesses excellent generalization capability and can reliably predict weld strain for parameter combinations outside the training domain. This performance is particularly noteworthy as it validates the model's practical applicability in real-world welding scenarios.

Overall Performance (R = 0.99891): The aggregate correlation coefficient of 0.99891 across all 20 experimental datasets provides compelling evidence of the ANN model's exceptional predictive power. The near-perfect alignment of data points along the 45-degree "Y = T" line in all four regression plots, with minimal scatter and no systematic deviations, confirms that the model captures the complex nonlinear relationships between welding parameters and strain without significant bias or error. The consistency of high R-values across all three data subsets—training, validation, and testing—provides robust statistical evidence that the developed ANN model is both accurate and reliable, making it a trustworthy predictive tool for weld strain estimation in engineering applications.

Based on the correlation coefficient (R) values shown in Figure 7, the network was deemed adequately trained and suitable for predicting weld strain from the input parameters, current (A), voltage (V), and gas flow rate (L/min).

The final phase involved testing the network's performance. For this, 15% of the input dataset (current, voltage, and gas flow rate) was fed into the trained model to generate predicted strain values. To assess prediction accuracy and reliability, a scatter plot was created in Microsoft Excel, with predicted strain on the vertical axis and observed (measured) strain on the horizontal axis, as presented in Figure 8. Network reliability was then quantified using the coefficient of determination (r^2) between the predicted and measured response values.

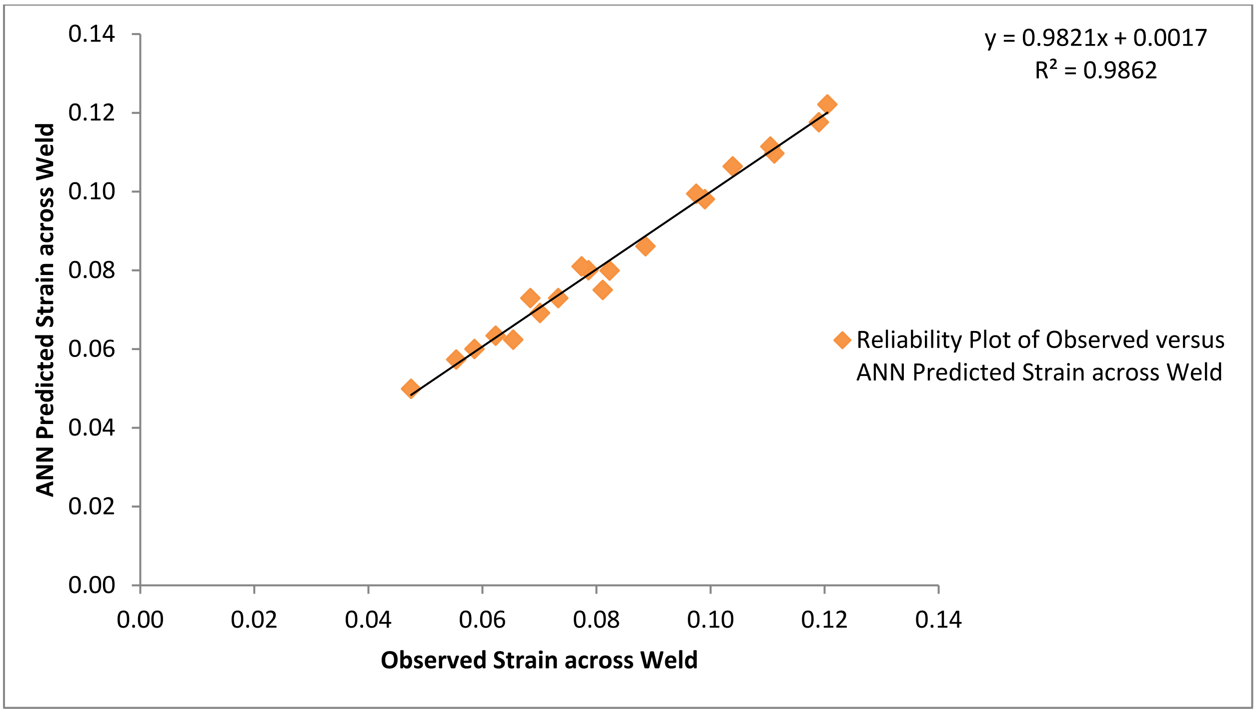

Figure 8: Reliability plot of observed versus ANN predicted strain across weld

The trained network was deemed effective for predicting thermal expansion coefficient, specific heat capacity, strain across welds, and lamellar tearing, based on the coefficient of determination (R2=0.9862$R2=0.9862$) observed for strain in Figure 8.

4.0 Conclusion

From the study, an optimized Artificial Neural Network model with ten hidden neurons trained using the Levenberg-Marquardt algorithm successfully predicted weld strain in ASTM A36 mild steel TIG welding from current, voltage, and gas flow rate inputs with exceptional accuracy ($R^2 = 0.9862$), demonstrating rapid convergence and strong generalization capability, thereby validating machine learning as a robust, cost-effective tool for welding process optimization and quality control.

The findings confirm that the systematic integration of central composite design for data generation, rigorous algorithmic selection, and architectural optimization yields a predictive framework that outperforms conventional experimental and computational approaches, offering weld engineers a practical solution for real-time strain prediction without recourse to time-consuming trials or intensive finite element analyses, while the established methodology and experimental dataset provide a valuable foundation for future research extending to other materials, welding processes, and multi-response prediction scenarios.

References

[1] Z. Mao, W. Liang, F. Yuan, and D. Deng, "Predicting welding deformation of mild steel bead-on-plate joints by means of artificial neural network and inherent strain method," *Journal of Manufacturing Processes*, vol. 142, pp. 424–439, Apr. 2025, doi: 10.1016/j.jmapro.2025.02.045.

[2] D. Deng and H. Murakawa, "FEM prediction of buckling distortion induced by welding in thin plate panel structures," *Computational Materials Science*, vol. 43, no. 4, pp. 591–607, Oct. 2008, doi: 10.1016/j.commatsci.2008.01.003.

[3] P. Dai, D. Mi, and B. Guo, "Bending deformation control in a laser-welded long straight structure by elastic pre-bending technique," *Journal of Manufacturing Processes*, vol. 107, pp. 485–495, Dec. 2023, doi: 10.1016/j.jmapro.2023.10.050.

[4] Z. Guo, H. Jiang, R. Bai, and Z. Lei, "Prediction of laser-welded deformation using artificial neural networks," *Journal of Laser Applications*, vol. 36, no. 1, Art. no. 012045, Feb. 2024, doi: 10.2351/7.0001256.

Received: 28/07/2026; Revised: 29/08/2026; Accepted: 31/08/2026; Published: 07/09/2026

[5] A. Hammad, C. Churiaque, and J. M. Sánchez-Amaya, "Experimental and numerical investigation of hybrid laser arc welding process and the influence of welding sequence on the manufacture of stiffened flat panels," *Journal of Manufacturing Processes*, vol. 61, pp. 527–538, Jan. 2021, doi: 10.1016/j.jmapro.2020.11.038.
[6] Y. Wang, G. Feng, and X. Pu, "Influence of welding sequence on residual stress distribution and deformation in Q345 steel H-section butt-welded joint," *Journal of Materials Research and Technology*, vol. 13, pp. 144–153, Jul. 2021, doi: 10.1016/j.jmrt.2021.04.061.
[7] J. Wang, N. Ma, and H. Murakawa, "An efficient FE computation for predicting welding induced buckling in production of ship panel structure," *Marine Structures*, vol. 41, pp. 20–52, Apr. 2015, doi: 10.1016/j.marstruc.2014.10.005.
[8] D. Deng, "Theoretical prediction of welding distortion in large and complex structures," *Frontiers of Materials Science in China*, vol. 4, pp. 202–209, Jun. 2010, doi: 10.1007/s11706-010-0017-7.
[9] Y. Ueda, K. Fukuda, and M. Tanigawa, "New measuring method of 3-dimensional residual stresses based on theory of inherent strain," *Journal of the Society of Naval Architects of Japan*, vol. 1979, no. 145, pp. 203–211, Jun. 1979, doi: 10.2534/jjasnaoe1968.1979.203.
[10] J. Wang, N. Ma, and H. Murakawa, "An efficient FE computation for predicting welding induced buckling in production of ship panel structure," *Marine Structures*, vol. 41, pp. 20–52, Apr. 2015, doi: 10.1016/j.marstruc.2014.10.005.
[11] D. Deng and H. Murakawa, "FEM prediction of buckling distortion induced by welding in thin plate panel structures," *Computational Materials Science*, vol. 43, no. 4, pp. 591–607, Oct. 2008, doi: 10.1016/j.commatsci.2008.01.003.
[12] D. Deng, H. Murakawa, and W. Liang, "Numerical simulation of welding distortion in large structures," *Computer Methods in Applied Mechanics and Engineering*, vol. 196, nos. 45–48, pp. 4613–4627, Sep. 2007, doi: 10.1016/j.cma.2007.05.023.
[13] W. Liang and D. Deng, "An inverse analysis method to estimate inherent deformations in thin plate welded joints," *Materials & Design*, vol. 88, pp. 1092–1101, Dec. 2015, doi: 10.1016/j.matdes.2015.09.105.
[14] J. Wang, L. Zhao, and D. Deng, "Influence of welding parameters on the inherent strain and welding distortion," *Marine Structures*, vol. 61, pp. 77–94, Sep. 2018, doi: 10.1016/j.marstruc.2018.05.002.
[15] W. Liang and D. Deng, "Influence of different constraint conditions on the inherent deformations of T-joints," *Journal of Materials Processing Technology*, vol. 264, pp. 489–501, Feb. 2019, doi: 10.1016/j.jmatprotec.2018.09.030.
[16] J. Wang, D. Deng, and H. Murakawa, "An empirical formula to calculate the tendon force of carbon steel at room temperature," *Marine Structures*, vol. 62, pp. 23–38, Nov. 2018, doi: 10.1016/j.marstruc.2018.07.008.
[17] W. Liang and D. Deng, "An inverse analysis method to estimate inherent deformations in thin plate welded joints," *Materials & Design*, vol. 88, pp. 1092–1101, Dec. 2015, doi: 10.1016/j.matdes.2015.09.105.
[18] J. Wang, D. Deng, and H. Murakawa, "Inherent deformation database of bead-on-plate joints and T-joints covering eight different materials," *Marine Structures*, vol. 73, Art. no. 102789, Sep. 2020, doi: 10.1016/j.marstruc.2020.102789.
[19] C. J. Barclay, A. S. Smith, and A. J. Pinkerton, "The application of artificial neural networks to the rectification of angular welding deformation," *Journal of Materials Processing Technology*, vol. 215, pp. 145–155, Jan. 2015, doi: 10.1016/j.jmatprotec.2014.08.006.
[20] Y. Rong, H. Zhang, and X. Wang, "Influence of bead profile on angular distortion of no gap butt joint by artificial neural network," *Journal of Manufacturing Processes*, vol. 42, pp. 145–155, Jun. 2019, doi: 10.1016/j.jmapro.2019.04.029.
[21] G. Christian, R. Kumar, and S. Chen, "ANN-based prediction of welding deformation and geometric accuracy for multilayer wire arc additive manufacturing structures," *Additive Manufacturing*, vol. 48, Art. no. 102429, Dec. 2021, doi: 10.1016/j.addma.2021.102429.
[22] C. Wu, J. Chen, and L. Zhang, "Welding sequence optimization framework based on back propagation neural network and artificial bee colony algorithm," *Journal of Manufacturing Processes*, vol. 58, pp. 1169–1181, Oct. 2020, doi: 10.1016/j.jmapro.2020.08.078.
[23] Y. Tian, R. Zhao, and H. Li, "Prediction of transverse shrinkage and angular deformation of TIG bead-on-plate joint using backward propagation neural network," *Journal of Materials Engineering and Performance*, vol. 29, pp. 2395–2406, Apr. 2020, doi: 10.1007/s11665-020-04764-x.
[24] J. Ren, Z. Zhang, and Q. Wang, "Multi-task learning ANN model for resistance spot welding process optimization," *Journal of Manufacturing Processes*, vol. 62, pp. 221–232, Feb. 2021, doi: 10.1016/j.jmapro.2020.12.041.
[25] S. Prak, K. Lee, and J. Kim, "Deep neural network for predicting residual stress at weld center and toe for butt joints," *Welding Journal*, vol. 100, no. 4, pp. 125–139, Apr. 2021, doi: 10.29391/2021.100.015.

[26] P. Lacki, A. Derlatka, W. Więckowski, and J. Adamus, "Development of FSW process parameters for lap joints made of thin 7075 aluminum alloy sheets," *Materials*, vol. 17, no. 3, Art. no. 672, Jan. 2024, doi: 10.3390/ma17030672.

[27] S. Arun Prakash and K. Gokul Kumar, "Failure evaluation on tailor made aerospace aluminum alloys via underwater friction stir welding employing predictive machine learning technologies," *Engineering Research Express*, vol. 6, no. 3, Art. no. 035405, Sep. 2024, doi: 10.1088/2631-8695/ad6d8f.

[28] M. A. Ben Messaoud, M. N. D. E. Cherief, and A. Miloudi, "Prediction and optimization of mechanical properties in FSWed AA6082-T6 joints using RSM and artificial neural networks," *The International Journal of Advanced Manufacturing Technology*, vol. 134, pp. 145–162, Jul. 2024, doi: 10.1007/s00170-024-14257-1.

[29] A. O. Igbinake, "Prediction of tensile strain in mild steel TIG weld using artificial neural networks," *UNIZIK Journal of Engineering and Applied Sciences*, vol. 5, no. 2, pp. 89–102, Mar. 2025, doi: 10.4314/ujeas.v5i2.8.

[30] J. Huo, X. Wang, and L. Zhang, "Prediction of mean strain from laser beam welding images and detection of defects via strain curves based on machine learning," *Optics and Laser Technology*, vol. 181, Art. no. 111849, Jun. 2025, doi: 10.1016/j.optlastec.2024.111849.